VISUAL SERVOING WITH ORIENTATION LIMITS OF A X4-FLYER

Najib Metni*, Tarek Hamel†, Isabelle Fantoni‡

*Laboratoire Central des Ponts et Chaussées, LCPC-Paris France, *najib.metni@lcpc.fr*
†Cemif-Sc FRE-CNRS 2494, Evry France, *thamel@iup.univ-evry.fr*
‡Heudiasyc UMR-CNRS 6599,Compiègne France, *Isabelle.Fantoni@hds.utc.fr*

Keywords: Unmanned Aerial Vehicle, Homography estimation, Visual Servoing, Nonlinear control.

Abstract

In this paper, we study the dynamics and the control using visual features of a four rotor vertical take-off and landing (VTOL) vehicle known as the X4-flyer while stabilizing with quasi-stationary flight above a planar target. A new control strategy is presented using the homography matrix, it is based on saturation functions for bounding the orientation of the UAV (unmanned air vehicle) in order to keep the target in the camera's field of view.

1 Introduction

Unmanned air vehicles (UAV) are becoming of a major interest in modern control theories. Several authors have contribution in the development of dynamic modelling [8, 6]. Their highly coupled dynamics and their small size provide an ideal testing ground for many complex control techniques. But the problem that arises in this kind of applications is the difficulty of measuring non-inertial variables as position, orientation, and linear velocity. One way of overcoming the problem is the use of vision sensor. Typically, a vision system onboard a UAV includes a Global Positioning System (GPS), an Inertial Navigation Sensor (INS) and a high-tech camera. So, almost all control strategies are built around a vision sensor. Indeed some works in the domain of control design, dedicated to helicopters, propose to use stereovision systems in the landing maneuvers of an UAV for the purpose of estimating the location and orientation of the helicopter landing pad. The vehicle considered in this paper is an autonomous hovering system, capable of quasi-stationary, vertical take-of and landing in near hover flight conditions.

All visual servoing techniques that involve reconstruction of the target pose with respect to the camera are called: *position based visual servoing* (PBVS). This kind of techniques lead to a Cartesian motion planning problem. Its main drawback is the need of a perfect knowledge of the target geometric model. The second class known as *image based visual servoing* (IBVS) aims to control the dynamics of features in the image plane directly [7]. Classical IBVS methods have the advantage of being robust with respect to calibration errors, however they suffer from the high coupling dynamics between translation and rotational motion which makes the cartesian trajectory uncontrollable. Recently, in [5] a new algorithm for visual servoing of an underactuated dynamic rigid body system, such a helicopter, based on exploiting the passivity-like properties of rigid body motion has been proposed. In this paper we use the method presented in [9] ($2\frac{1}{2}$D visual servoing) that consists of combining visual features obtained directly from the image, and features expressed in the Euclidean space. More precisely, a homography matrix is estimated from the planar feature points extracted from the two images (corresponding to the current and desired poses). From the homography matrix, we will estimate the relative position of the two views.

The purpose of this paper is to study how we can use the approach given in [9] to control an autonomous hovering system. First, we propose a simplified dynamic model of a four-rotor vertical take-off and landing (VTOL) vehicle known as the X4-flyer. Then we propose a control design based on separating the translational from the rotational rigid body (airframe) dynamics [6]. The control strategy is new because it takes into account a limit for the orientation of the X4-flyer in order to keep the target in the camera's field of view. We will prove the stability of such strategy based on saturation functions.

2 The X4-flyer dynamic model

The X4-flyer is a system consisting of four individual electric fans, linked to a rigid cross frame as shown in Figure 1. It operates as an omnidirectional UAV. Vertical motion is controlled by collectively increasing or decreasing the power of all four motors. Lateral motion is achieved by controlling differentially the motors generating a pitch/roll motion of the airframe that inclines the collective thrust and leads to lateral acceleration. Yaw control is derived from the reactive couple applied to the airframe due to rotor drag. Diagonally opposite rotors turn in opposite directions (cf. Fig. 1) leading to a balanced torque distribution in hover conditions. To apply yaw control, the speed of a pair of diagonal motors is increased while it is decreased in the opposing pair. This generates a torque around the vertical axis while maintaining the total thrust.

Let $F^* = \{E_x, E_y, E_z\}$ denote a right-hand inertial or world frame such that E_z denotes the vertical direction downwards into the earth. Let $\xi = (x, y, z)$ denote the position of the centre of mass of the object in the frame F^* relative to a fixed origin in F^*. Let $F = \{E_1^a, E_2^a, E_3^a\}$ be a (right-hand) body fixed frame for the airframe. The orientation of the airframe is given by a rotation $R : F \to F^*$, where $R \in SO(3)$ is an orthogonal

Figure 1: A prototype X4-flyer.

rotation matrix.

Let $V \in F$ denote the linear velocity and $\Omega \in F$ denote the angular velocity of the airframe both expressed in the body fixed frame. Let m denote the mass of the rigid object and let $\mathbf{I} \in \Re^{3\times 3}$ be the constant inertia matrix around the centre of mass (expressed in the body fixed frame F). Newton's equations of motion yield the following dynamic model for the motion of a rigid object:

$$\dot{\xi} = RV \tag{1}$$

$$m\dot{V} = -m\Omega \times V + \mathcal{F} \tag{2}$$

$$\dot{R} = R\text{sk}(\Omega), \tag{3}$$

$$\mathbf{I}\dot{\Omega} = -\Omega \times \mathbf{I}\Omega + \Gamma. \tag{4}$$

The notation $\text{sk}(\Omega)$ denotes the skew-symmetric matrix such that $\text{sk}(\Omega)v = \Omega \times v$ for the vector cross-product $\times$ and any vector $v \in \Re^3$. The vector forces and the vector torques are described as follows

$$\mathcal{F} = mgR^T e_3 - u_4 e_3 \tag{5}$$

$$\Gamma = u_1 e_1 + u_2 e_2 + u_3 e_3 \tag{6}$$

In the above notations, g is the acceleration due to gravity. The inputs (u_1, u_2, u_3, u_4) are derived from the individual motor control signals (cf. [4]).

3 Motion Estimation

3.1 Camera Projection and Planar Homography

Visual data is obtained via a projection of real world images onto the camera image surface. This projection is parameterized by two sets of parameters: intrinsic (i.e., those "internal" parameters of the camera such as the focal length, the pixel aspect ratio etc.) and extrinsic (the pose - position and orientation of the camera). The pose of the camera determines a rigid body transformation from the world or inertial frame F^* to the camera fixed frame F (and vice-versa). One has

$$P^* = RP + \xi \tag{7}$$

as a relation between the coordinates of the same point in body fixed frame ($P \in F$) and in the world frame ($P^* \in F^*$).

Let p is the image of the point P^* and p^* is the image of the same point viewed when the camera is aligned with frame F^* (see fig.2). When all target points lie in a single planar surface one has

$$P_i = R^T P_i^* + \frac{tn^{*T}}{d^*} P_i^*, \quad i = 1, \ldots, k, \tag{8}$$

and thus the projected points obey [1]

$$p_i \cong \left(R^T + \frac{tn^{*T}}{d^*} \right) p_i^*, \quad i = 1, \ldots, k. \tag{9}$$

The projective mapping $H := \left(R^T + \frac{tn^{*T}}{d^*} \right)$ is called a homography matrix, it relates the images of points on a target plane when viewed from two different poses (defined by the coordinate systems F and F^*). More details on the homography matrix could be found in [4]. The homography matrix contains the pose information (R, ξ) of the camera. However, since a projective relationship exists between the image points and the homography, it is only possible to determine H (using only image points equations) up to a scale factor. There are numerous approaches for determining H, up to this scale factor, cf. for example [1].

Extracting R and $\frac{t}{d^*}$ from H can be quite complex [9, 13, 12, 3]. However, one quantity $r = \frac{d}{d^*}$ can be calculated easily and directly:

$$r = 1 + \frac{n^T t}{d^*} = \det(H) = \det(R^T + \frac{tn^{*T}}{d^*}).$$

There are certain special cases where it is relatively straight forward to compute important parameters from an unscaled estimate of the homography matrix H. An important case is where the target plane is perpendicular to the line of sight of the world frame ($n^* = (0, 0, 1)^T$). In this case, the first two columns of H are scaled versions of the first two columns of R. This special case is particularly useful in stabilizing a UAV over a landing pad, as long as the camera is mounted beneath the vehicle so as the line of sight is vertically downward. This case will be used in the simulation (section 4).

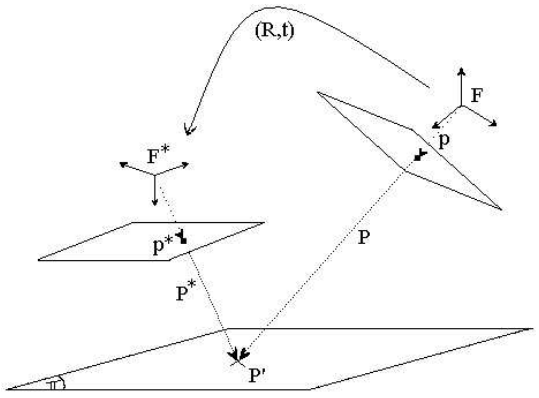

Figure 2: Camera projection diagram showing the desired (F^*) and the current (F) frames

3.2 Visual servoing control strategy

In this section, visual servoing is based on Lyapunov control design and on saturation functions. By exploiting equations (1)-

[1] Most statements in projective geometry involve equality up to a multiplicative constant denoted $\cong$.

(4), we derive a control strategy for limiting the robot orientation.

To simplify the derivation, it is assumed that the camera fixed frame coincides with the body fixed frame F.

Let P' denote the observed point of reference of the planar target, and P^* be the representation of P' in the camera fixed frame at the desired position (Figure 2). The dynamics associated with the stabilization of the camera around the desired position P^* fully determine two degrees of freedom (pitch and roll) in the attitude of the airframe. The yaw of the airframe must be separately assigned. In this paper we use the classical 'yaw', 'pitch' and 'roll' Euler angles (ϕ, θ, ψ) commonly used in aerodynamic applications [10]. Although these angles are not globally defined they provide a suitable local representation for all quasi-stationary manoeuvres undertaken by an X4-flyer. The yaw angle trajectory is specified directly in terms of the angle ϕ_d, the desired yaw angle. The relationship between the Euler angles used and the rotation matrix is[2]

$$R = \begin{pmatrix} c_\theta c_\phi & s_\psi s_\theta c_\phi - c_\psi s_\phi & c_\psi s_\theta c_\phi + s_\psi s_\phi \\ c_\theta s_\phi & s_\psi s_\theta s_\phi + c_\psi c_\phi & c_\psi s_\theta s_\phi - s_\psi c_\phi \\ -s_\theta & s_\psi c_\theta & c_\psi c_\theta \end{pmatrix}. \quad (10)$$

The visual servoing problem considered is:

Find a smooth state feedback (u_1, u_2, u_3, u_4) depending only on the measurable states (the observed point p,the homography matrix H, the translational and angular velocities (V, Ω), and the estimated parameters (R,r) from the homography matrix (H) which provide a partial pose estimation), such that the following error

$$(\epsilon = R(P - R^T P^*), \quad \sigma = \phi - \phi_d)$$

is asymptotically stable.

Note: ϵ and σ are not defined in terms of visual information. In the sequel, these errors will be transformed to quantities that are expressed in terms of visual information.

Recall that the current and desired position P and P^* of the observed point are not known and the only information that we have are given by their projections, the estimated matrix R and the ratio, r, between the distances d and d^* which is given by the determinant of the homography matrix H.

Following [9], the camera can be controlled in the image space and in the Cartesian space at the same time. They propose the use of three independent visual features, such as the image coordinates of the target point associated with the ratio r delivered by determinant of the homography matrix. Consequently, let us consider the reference point P' lying in the reference plan π and define the scaled cartesian coordinates using visual information as follow:

$$P_r = \frac{{n^*}^T p^*}{n^T p} rp$$

[2]The following shorthand notation for trigonometric function is used:

$$c_\beta := \cos(\beta), \quad s_\beta := \sin(\beta), \quad t_\beta := \tan(\beta).$$

Knowing that

$$\frac{||P||}{||P^*||} = \frac{{n^*}^T p^*}{n^T p} r,$$

it follows that we can reformulate the error ϵ in terms of available information

Let us define

$$\epsilon_1 = R\left(\frac{{n^*}^T p^*}{n^T p} rp - R^T p^*\right) \quad (11)$$

From the above discussion and equations describing the system dynamics, the full dynamics of the error ϵ_1 may be rewritten as

$$\dot{\epsilon}_1 = \frac{1}{||P^*||} v \quad (12)$$

$$m\dot{v} = -u_4 R e_3 + mg e_3 \quad (13)$$

$$\dot{R} = R\text{sk}(\Omega) \quad (14)$$

$$\mathbf{I}\dot{\Omega} = -\Omega \times \mathbf{I}\Omega + \Gamma \quad (15)$$

Define

$$\delta := \epsilon_1 + v \quad (16)$$

Let S_1 be the first storage function for the backstepping procedure. It is chosen for the full linear dynamics Eqn's 12-13

$$S_1 = \frac{1}{2}||\delta||^2 + \frac{1}{2}||v||^2 \quad (17)$$

Taking the time derivative of S_1 and substituting for Eq. 12 and 13 yields

$$\frac{d}{dt} S_1 = \rho \delta^T v + (\delta + v)^T (mg e_3 - u_4 R e_3) \quad (18)$$

where $\rho = \frac{1}{||P^*||}$.

Applying classical backstepping one would assign a virtual vectorial control for $\frac{1}{m}(u_4 R e_3)^d$

$$u_4 (R e_3)^d := mg e_3 + mv + m\delta \quad (19)$$

This choice is sufficient to stabilize S_1 if the term $(u_4 R e_3)^d$ were available as a control input. If $u_4 R e_3$=$(u_4 R e_3)^d$ then

$$\dot{S}_1 = -||\delta||^2 - (2 - \rho)\delta^T v - ||v||^2$$

is negative definite $\forall \rho < 1$.

Note that the vectorial input can be split into its magnitude u_4, that is linked directly to the motor torques, and its virtual (or desired) direction $R_d e_3$, that defines two degrees of freedom in the airframe attitude dynamics (Eqn's 14-15). In this case, the magnitude and its virtual (or desired) direction of the vectorial term become:

$$|u_4| = ||mge_3 + mv + m\delta||; \quad R_d e_3 = \frac{mge_3 + mv + \delta}{|u_4|} \quad (20)$$

Now, to determine the fully desired rotation matrix R_d we have to find the constraint of the yaw parameter using another vector. Let e_1 be the desired orientation. We define the vector σ which belongs to the plane built by the two vectors e_1 and $R_d e_3$ ($\sigma \in span\{R_d e_3, e_1\}$) and we impose that $\sigma = R_d e_1$ (by this way, σ will be perpendicular to $R_d e_3$). We obtain

$$\sigma = \frac{e_1 + \alpha R_d e_3}{||e_1 + \alpha R_d e_3||}; \quad \text{with } \sigma^T R_d e_3 = 0 \quad (21)$$

Here α is a real number obtained by solving the two above equations. The final equation for the desired matrix R_d can be defined as:

$$R_d = [\sigma \quad \sigma \wedge (R_d e_3) \quad R_d e_3] \quad (22)$$

3.2.1 Limiting The X4-flyer Orientation

In the theoretical developments based on the backstepping (see [5]), the proposed law of control assures an exponential convergence towards the desired position. It seems to us, however, that this type of convergence is not recommended when the vehicle is initially far from this position. Indeed, the dynamic model based on quasi-stationary conditions (hover conditions) is not valid anymore, because the dynamics of such a convergence will provoke a different flight mode. Moreover, the target image may leave the field of view of the camera during the evolution of the vehicle. To avoid such situations, it is necessary to insure that the focal axis of the camera is close to the gravity direction. In the sequel, we propose to use small gains technique (for example the technique of saturation functions presented by Teel in [11]). This technique seems well adapted to our problem. Indeed, if the orientation is saturated, we can insure that the X4-flyer will remain in quasi-stationary manoeuvres during all the operation.

The orientation $R_d e_3$ is a function of the terms v and δ. In order to limit the orientation, we add a saturation on the two terms v and δ. Therefore, Eq. 19 becomes

$$u_4 R_d e_3 = mge_3 + m\ \text{Sat}_2(v + \text{Sat}_1(\delta)) \quad (23)$$

where $\text{Sat}(x)$ is a continuous, nondecreasing saturation function satisfying:

- $x^T \text{Sat}_i(x) > 0$ for all $x \neq 0$.
- $\text{Sat}_i(x) = x$ when the components of the vector x are smaller than L_i ($|x_{(.)}| \leq L_i$.
- $|\text{Sat}_i(x)| \leq M_i$ for all $x \in \mathbb{R}$.

Proposition 3.1 *The following choice of the saturation functions [11]*

$$M_i < \frac{1}{2} L_{i+1}; \quad \frac{1-\rho}{2} L_{i+1} \leq L_i \leq M_i$$

ensures global stabilization of the linear dynamics when equation 23 is used as control input of the translational dynamics

Proof Recalling Eq. 13 and Eq. 23, it yields

$$\dot{v} = -\text{Sat}_2(v + \text{Sat}_1(\delta))$$

Consider the storage function $S_v = \frac{1}{2}||v||^2$. The derivative of S_v is given by

$$\dot{S}_v = -v^T \text{Sat}_2(v + \text{Sat}_1(\delta))$$

Using conditions on Sat_i coupled with the fact that $M_1 \leq L_2$, it follows that $\dot{S}_v < 0$ ($\forall |v_{(.)}| \geq \frac{1}{2} L_2$) ($v_{(.)}$ represents a component of the vector v). Consequently, it exist a finite time T_1 after which all components of the linear velocity vector $v_{(.)} \leq \frac{1}{2} L_2$ ($\forall t \geq T_1$). The control law Eq. 23 becomes then

$$u_4 R_d e_3 = mge_3 + m(v + \text{Sat}_1(\delta)), \quad \forall t \geq T_1$$

Now consider the evolution of the term δ for $t \geq T_1$. Let S_δ the storage function associated with the term δ ($S_\delta = \frac{1}{2}||\delta||^2$). Deriving S_δ it yields

$$\dot{S}_\delta = \delta^T ((\rho - 1)v - \text{Sat}_1(\delta))$$

Using the second condition of the proposition, one can observe that the components of the vector δ become smaller than M_1 after a finite time T_2. After T_2, the control law becomes

$$u_4 R_d e_3 = mge_3 + m(v + \delta), \quad \forall t \geq T_2$$

insuring exponential stability after the time T_2. $\triangle$

Using the saturated control law (Eq. 23), the derivative of the first storage function becomes

$$\dot{S}_1 = -||\delta||^2 - (2-\rho)\delta^T v - ||v||^2 - (\delta + v)^T |u_4|^s (\tilde{R} - I) R_d e_3$$

where

$$\tilde{R} = R R_d^T; \quad \text{and } |u_4|^s = ||mge_3 + m\ \text{Sat}_2(v + \text{Sat}_1(\delta))||$$

According to the above proposition, the system with such a saturated input is globally asymptotically stable if the new error term $\tilde{R} - I$ converges to zero. Now, it only remains to control the attitude dynamics involving the error $\tilde{R} - I$.

3.2.2 Attitude dynamics control

The next step of the control design involves the control of the attitude dynamics such that the error $\tilde{R} - I$ converges exponentially to zero. We will use a quaternion representation of the rotation to obtain a smooth control for $\tilde{R}$. The attitude deviation $\tilde{R}$ is parameterized by a rotation $\tilde{\gamma}$ around the unit vector $\tilde{k}$. Using Rodrigues' formula ([10]) one has

$$\tilde{R} = I + \sin(\tilde{\gamma})\text{sk}(\tilde{k}) + (1 - \cos(\tilde{\gamma}))\text{sk}(\tilde{k})^2$$

The quaternion representation describing the deviation $\tilde{R}$ is given by [2]

$$\tilde{\eta} := \sin\frac{\tilde{\gamma}}{2}\tilde{k}, \qquad \tilde{\eta}_0 := \cos\frac{\tilde{\gamma}}{2}; \;\; \text{with} \;\; ||\tilde{\eta}||^2 + \tilde{\eta}_0^2 = 1$$

The deviation matrix $\tilde{R}$ is then defined as follows

$$\tilde{R} = (\tilde{\eta}_0^2 - ||\tilde{\eta}||^2)I + 2\tilde{\eta}\tilde{\eta}^T + 2\tilde{\eta}_0 \text{sk}(\tilde{\eta}) \tag{24}$$

The attitude control control objective is to achieve when $\tilde{R} = I$. From Eqn 24 this is equivalent to $\eta = 0$ and $\tilde{\eta}_0 = 1$. Indeed, it may be verified that

$$||\tilde{R} - I||_F = \sqrt{\text{tr}((R-I)^T(\tilde{R}-I))} = 2\sqrt{2}||\tilde{\eta}|| \tag{25}$$

Based on this result, the attitude control objective is to drive $\tilde{\eta}$ to zero. Differentiating (η, η_0) yields (see [10])

$$\dot{\tilde{\eta}} = \frac{1}{2}(\tilde{\eta}_0 I + \text{sk}(\tilde{\eta}))\tilde{\Omega}, \qquad \dot{\tilde{\eta}}_0 = -\frac{1}{2}\tilde{\eta}^T\tilde{\Omega} \tag{26}$$

where $\tilde{\Omega}$ denotes the error angular velocity

$$\tilde{\Omega} = R_d(\Omega - \Omega_d) \tag{27}$$

and Ω_d represents the desired angular velocity. In order to find the desired angular velocity, we have to consider the time derivative of the desired orientation $R_d e_3$

$$\dot{R}_d = R_d \text{sk}(\Omega_d); \;\; \dot{R}_d e_3 = R_d e_3 \text{sk}(\Omega_d) \tag{28}$$

Since differentiating the expression of $R_d e_3$is quite complex, so we will design a control law with a high gain virtual control $\tilde{\Omega}^v$. In this way we can neglect the time derivative of $R_d e_3$.

Then, by choosing the virtual control as

$$\tilde{\Omega}^v \approx \Omega^v = -2k\tilde{\eta}_0\tilde{\eta}$$

with parameter k chosen high enough to neglect Ω_d. With the above choice, we then have

$$\dot{\tilde{\eta}} = -\frac{k}{2}||\tilde{\eta}_0||^2\tilde{\eta} + \frac{k}{2}\tilde{\eta}_0 R_d\nu + k\text{sk}(\tilde{\eta})R_d\nu$$

where

$$\nu := \frac{1}{k}\Omega + R_d^T\tilde{\eta}_0\tilde{\eta} \tag{29}$$

and its time derivative $\dot{\nu}$ is given by

$$\dot{\nu} = \frac{\dot{\Omega}}{k} + \chi \tag{30}$$

where

$$\chi = \frac{1}{2}R_d^T\tilde{\eta}^T R_d\Omega\tilde{\eta} + R_d^T\tilde{\eta}_0(\frac{1}{2}\tilde{\eta}_0 I + \text{sk}(\tilde{\eta}))R_d\Omega \tag{31}$$

The time derivative of ν becomes

$$\dot{\nu} = -\frac{k}{2}\tilde{\eta}_0 R_d^T\tilde{\eta} - \frac{k}{2}||\tilde{\eta}_0||^2\nu \tag{32}$$

Let us define the Lyapunov function candidate for the attitude deviation :

$$S_2 = \frac{1}{2}||\tilde{\eta}||^2 + \frac{1}{2}||\nu||^2. \tag{33}$$

Taking the time derivative of S_2 and using (32), we obtain

$$\dot{S}_2 = -\frac{k}{2}||\tilde{\eta}_0||^2||\tilde{\eta}||^2 - \frac{k}{2}||\tilde{\eta}_0||^2||\tilde{\nu}||^2 \tag{34}$$

This completes the control design for the attitude dynamics, since the time derivative of the storage function in (34) is definite negative. Then the input of the new control law (eq. 23) limiting the orientation ensures the exponential stability of the system.

4 Simulation results

In order to evaluate the efficacy of the proposed servoing technique with orientation limits, simulation results which concerns the above "X4-flyer" model are presented. The experiment considers a basic stabilization. The target is five points: four on the vertices of a planar square and one on its center (see the initials points on fig 4). The available signals are the pixel coordinates of the five points observed by the camera.

For this experiment, it is assumed that the plane is perpendicular to the line of sight (*i. e.* the unit vector normal to the target plane is equal to the direction of the gravity $n^* = e_3$)

As discussed in the end of section 3.1 the homography matrix has two columns of a rotation matrix R^T as the first two columns. The desired image feature is chosen such that the camera set point is located some meters above the square.

Using the above specification, the error ϵ_1 (eq.11) is defined as follows

$$\epsilon_1 = \frac{1}{n^T p}rp - R^T e_3$$

The parameters used for the dynamic model are $m = 0.6$, $\mathbf{I} = \text{diag}[0.4, 0.4, 0.6]$, $g = 10$, $d = 0.25$ and $\kappa = 0.01$. Initially, the X4-flyer is assumed to hover at some meters above the ground with thrusts corresponding to necessary forces to maintain stationary flight $u_4 \approx mg$.

For the sake of the simulation, the initial position of the X4-Flyer is $x = 10$, $y = 15$, $z = -12$. Its orientation is fixed as the identity matrix I_3 and it is considered also in hover conditions ($\Omega = 0$). The simulation is presented to validate the proposed control design. It simulates the behavior of the X4-flyer dynamics in the ideal case (extraction of the homography matrix without disturbance). We will compare the results of the new control law (with orientation limits) versus the evolution of the states in the control law (without orientation limits) developed in [4] (Figure 3). One can notice that the time of convergence

for the states following the new law of control is longer than the previous law, but instead we see that the variation of the Euler angles are restricted to small values (in this case, in the order of 10^{-3}rad). So the new control law which limits the X4-flyer orientation ensures small values for Euler angles, therefore we are sure that the dynamics of the flying vehicle are applicable to the hover conditions (quasi-stationary manoeuvres) and the object will remain in the field of view of the camera. Finally, Figure 4 shows us the evolution of the target from the initial position till the desired position (highlighted by the dashed square).

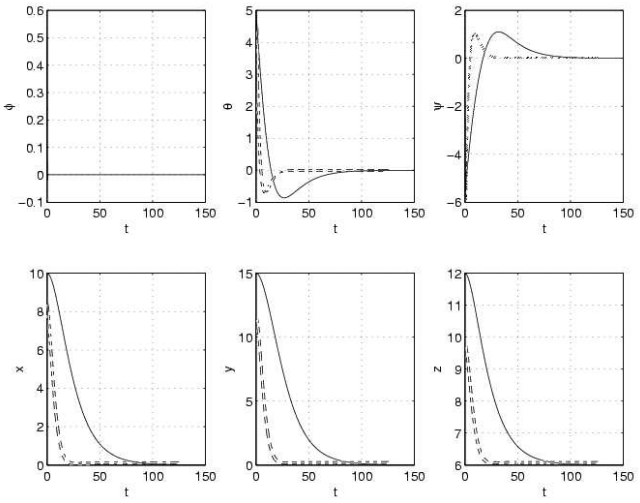

Figure 3: Evolution of the "X4-flyer" states (the 3 Euler Angles [radian] and the 3 coordinates [meter]) in the 2 control laws: without limiting its orientation (Dashed Lines-Angles in 10^{-1}rad), and the new control law (Full Lines-Angles in 10^{-3}rad)

5 Conclusion

In this paper, we presented a control strategy for the autonomous flight of the X4-flyer taking into account an orientation limit in order to keep the image in the camera's view field.

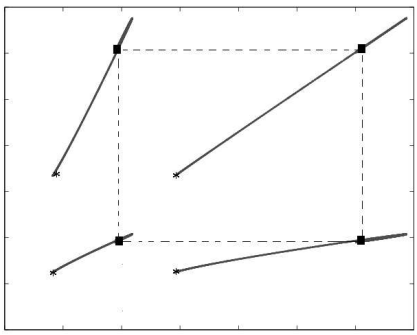

Figure 4: Evolution of the target points in the image surface for the new control law. Points evolving from initial position till the desired position (dashed square)

The control strategy is based on separating the airframe dynamics from the motor dynamics. This strategy only requires that the system is able to measure–with a video camera– the image plane mapping features on a planar surface (such as a landing pad).

References

[1] B. Couapel and B. Bainian. Stereo vision with the use of a virtual plane in the space. *Chinese Journal of Electronics*, 4(2):32–39, Avril 1995.

[2] O. Egeland, M. Dalsmo, and O.J. Sordalen. Feedback control of a nonholonomic underwater vehicle with constant desired configuration. *Int. Journal of Robotics Research*, 15:24–35, 1996.

[3] O. Faugeras and F. Lustman. Motion ans structure from motion in a piecewise planar environment. *International Journal of Pattern Recognition and Artificial Intelligence*, 2(3):485–508, 1988.

[4] T. Hamel, D.Suter, and R. Mahony. Visual servoing based on homography estimation for the stabilization of an x4-flyer. 2002.

[5] T. Hamel and R. Mahony. Visual servoing of under-actuated dynamic rigid body system : An image space approach. In *39th Conference on Decision and Control*, 2000.

[6] T. Hamel, R. Mahony, R. Lozano, and J. Ostrowski. Dynamic modelling and configuration stabilization for an x4-flyer. In *15th IFAC World Congress*, 2002.

[7] S. Hutchinson, D. Ager, and P.I. Cake. A tutorial on visual servo control. In *IEEE Trans. on Robotics and Automation*, volume 12, Octobre 1996.

[8] Y. Ma, S. Sastry, and J. Kosecka. View recovery from image sequences: Discrete viewpoint vs. differential viewpoint. Electronic research laboratory memorandum, UC, Berkeley, 1997.

[9] E. Malis. *Contribution à la modélisation et à la commande en asservissement visuel*. PhD thesis, Université de Rennes, 1998.

[10] R.M. Murray, Z. Li, and S. Sastry. *A mathematical introduction to robotic manipulation*. CRC Press, 1994.

[11] A.R. Teel. Global stabilization and restricted tracking for multiple integrators with bounded controls. *System and Control Letters*, 18:165–171, 1992.

[12] J. Weng, T.S. Huang, and N. Ahuja. Motion and structure from line correspondences: Closed-form solution, uniqueness, and optimization. 1992.

[13] Z. Zhang and A.R. Hanson. Scaled euclidean 3d reconstruction based on externally uncalibrated cameras. In *IEEE Symposium on Computer Vision*, Coral Glabes, Floride, 1995.